University of Szeged
Department of Mathematics

Biomathematics of *Chlamydia* PhD Thesis Booklet

Bornali Das

Supervisor: Gergely Röst

1 Introduction

Chlamydia trachomatis (*C. trachomatis*) is a bacterium that belongs to *Chlamydia*, a genus of pathogenic gram-negative bacteria which are obligate intracellular parasites. *C.trachomatis* typically affects humans and is reportedly the most common STI worldwide. It causes diseases in humans by infecting the genital tract and ocular epithelium [1]. A report on the global incidence and prevalence of selected curable STIs in the year 2008 reported 105.7 million cases of *C. trachomatis* [2]. The Centers for Disease Control and Prevention (CDC) reports that there are 4 million new instances of *C. trachomatis* infections in the United States each year. Moreover, it is overtly distressing that young people between 15-24 are primarily affected, marking up to 50% of new STIs occurring each year [3].

1.1 Life Cycle of *Chlamydia*

Chlamydia's unique biphasic intracellular developmental cycle differs from other bacterial parasites. They manifest in two morphologically distinct forms within the host: the elementary bodies (EBs) and the reticulate bodies (RBs). The EBs are the extracellularly viable, but metabolically inert forms, responsible for spreading the infection by attaching and invading susceptible epithelial human cells. RBs are metabolically active non-infectious forms that can replicate inside human cells. The life cycle of *Chlamydia* is initiated when the EBs attach themselves to the surface of the host epithelial cell; followed by the internalization into an intracytoplasmatic parasitophorous vacuole called inclusion, whereby they undergo morphological changes and differentiate into the replicative form RBs. The RBs then multiply by undergoing repeated cycles of binary fission (200-500 fold; [4]). Matured RBs then differentiate back to EBs and are eventually released at the end of the cycle with the lysis of the infected host cell [5].

As it stands, the fact that *Chlamydia*'s developmental forms exclusively alternates between EB and RB has been oversimplified. Interestingly, *Chlamydia* can enter a non-infectious yet viable stage known as persistence when under stress despite being efficiently treatable. Persistence in *Chlamydia* is a reversible phase that is characterized by an anomalous development cycle where the bacteria is capable of establishing latent infections and can persist asymptomatically in many individuals [6]. Unresolved *Chlamydia* infections leading to the persistence of the bacteria are believed to be a principal reason behind recurrent *Chlamydia* diseases.

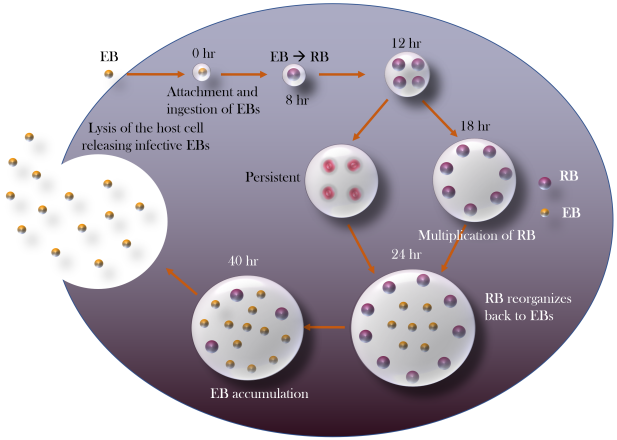

Figure 1.1: Graphical representation of the *Chlamydia* development cycle in the presence of persistence. Arrows indicate transition from one stage to another.

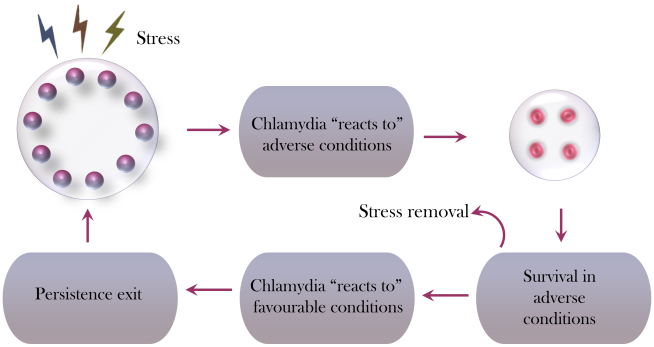

Figure 1.2: The persistence phenomenon.

2 Delay linear chains in mathematical biology: An insight into the intracellular *Chlamydia* infection

We develop a linear system of delay differential equations that is applicable to the mathematical representation of some compartmental models in biology and ecology. Consider a delayed linear chain as shown in Figure 2.1, illustrating particles moving through a number of successive compartments before reaching a final stage. The multiplicative rates represent growth between the compartments. All the compartments have inflow and outflow terms except the first and the last: the first compartment has only outflow and the last compartment has only inflow. Time delay signifies the time needed to complete the transition of particles between successive compartments.

Let the number of particles in the ith compartment at time t be $y_i(t)$ ($i = 0, 1, \ldots, n$). The rate at which the particles are moving out of the ith compartment is denoted by a_i for $i = 0, 1, \ldots, n-1$ and b_{i-1} is the rate at which the particles are entering the ith compartment for $i = 1, 2, \ldots, n$. Also, we assume that the particles are arriving with a time delay τ_{i-1} into the ith compartment for $i = 1, 2, \ldots, n$. We describe such a process by a system of delay differential equations as follows:

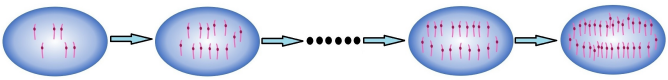

Figure 2.1: Schematic diagram of a linear chain.

$$\begin{cases} y_0'(t) &= -a_0 y_0(t), \\ y_i'(t) &= b_{i-1} y_{i-1}(t-\tau_{i-1}) - a_i y_i(t), \qquad i = 1, 2, \ldots, n-1, \\ y_n'(t) &= b_{n-1} y_{n-1}(t-\tau_{n-1}), \end{cases} \tag{2.1}$$

where $a_i > 0$, $b_i > 0$ and $\tau_i \geq 0$ for all i. The natural phase space for our system is $C([-\tau, 0], \mathbb{R}^{n+1})$, where $\tau = \max\{\tau_0, \ldots, \tau_{n-1}\}$. Initial conditions for this system are given by

$$y_i(\theta) = \varphi_i(\theta) \text{ for } \theta \in [-\tau, 0], i = 0, \ldots, n \tag{2.2}$$

where $\varphi := (\varphi_0, \ldots, \varphi_n) \in C([-\tau, 0], \mathbb{R}_+^{n+1})$.

It is well known that the initial value problem Eq. (2.1)-Eq. (2.2) is well-posed. Non-negativity of the initial data is a natural requirement for the biological systems we consider, and from the non-negativity of the rates, it follows that solutions remain non-negative for all future time. In the following proposition, an explicit expression for the limit of each compartment is given.

Proposition 2.0.1. *Solutions of problem (Equation* (2.1)*) has the following limits:*

$$\lim_{t\to\infty} y_i(t) = 0 \text{ for } i = 0, 1, 2, \ldots, n-1$$

and

$$\begin{aligned}\lim_{t\to\infty} y_n(t) = {} & \frac{b_0 \ldots b_{n-1}}{a_0 \ldots a_{n-1}}\varphi_0(0) + \frac{b_1 \ldots b_{n-1}}{a_1 \ldots a_{n-1}}\varphi_1(0) + \cdots + \frac{b_{n-1}}{a_{n-1}}\varphi_{n-1}(0) \\ & + \varphi_n(0) + \frac{b_0 \ldots b_{n-1}}{a_1 \ldots a_{n-1}}\int_{-\tau_0}^{0} \varphi_0(s)ds + \frac{b_1 \ldots b_{n-1}}{a_2 \ldots a_{n-1}}\int_{-\tau_1}^{0} \varphi_1(s)ds \\ & + \cdots + \frac{b_{n-2}b_{n-1}}{a_{n-1}}\int_{-\tau_{n-2}}^{0} \varphi_{n-2}(s)ds + b_{n-1}\int_{-\tau_{n-1}}^{0} \varphi_{n-1}(s)ds.\end{aligned}$$

2.1 Mathematical Formulation of the Intracelluler *Chlamydia* Development Cycle

In this section, we construct a mathematical model for a laboratory experiment of *Chlamydia* infecting human cells [7]. In the absence of persistence, the life cycle alternates between the EBs and the RBs.

Variables	Descriptions
$y_0(t)$	Number of EBs outside human cells at time t
$y_1(t)$	Number of EBs attached to human cells at time t.
$y_2(t)$	Number of EBs that have transformed to RBs,
$y_i(t)$	Number of RBs after the ith cycle of replication for $i = 3, 4, \ldots, n-1$.
$y_n(t)$	Number of RBs converting back to EBs.

Table 2.1: Variables and their Descriptions

According to certain assumptions, and description of variables given in Table 2.1, the population dynamics of EBs and RBs can be described in mathematical terms as follows:

$$\begin{cases} y_0'(t) &= -a_0 y_0(t), \\ y_1'(t) &= a_0 y_0(t-\tau_0) - a_1 y_1(t), \\ y_2'(t) &= a_1 y_1(t-\tau_1) - a_2 y_2(t), \\ y_i'(t) &= 2a_{i-1} y_{i-1}(t-\tau_{i-1}) - a_i y_i(t), \qquad i = 3, 4, .., n-1 \\ y_n'(t) &= a_{n-1} y_{n-1}(t-\tau_{n-1}). \end{cases} \tag{2.3}$$

In consistency with the laboratory experiment [7], we have the initial conditions

$$\begin{cases} y_0(0) &= 100, \\ y_0(t) &= 0, \qquad \text{for } t < 0, \\ y_i(t) &= 0, \qquad \text{for } t \leqslant 0, \quad \text{where} \quad i = 1, 2, \ldots, n. \end{cases} \tag{2.4}$$

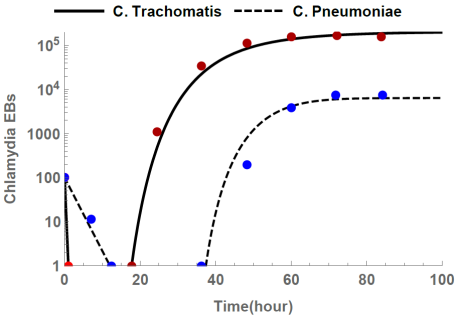

Figure 2.2: Model-based curves after parameter fitting. The colored dots are taken from laboratory measurements. It shows the growth cycle of two different strains of *Chlamydia* bacteria, the fast-replicating *C. trachomatis* and slow-replicating *C. pneumoniae* as reflected in the figure.

Here, a_0 is the rate at which the EBs enter the human cell and they are assumed to differentiate to RBs at a rate a_1 inside the human cells. Parameter a_{i-1} is the rate at which the RBs enter the ith cycle of replication for $i = 3, 4, \ldots, n-1$, and the RBs will convert back to the EBs with the rate a_{n-1}. As in the previous two cases, we can have equations for the number of cells undergoing transformation or differentiation, but since the equations decouple from the rest, we ignore them in this case too.

Proposition 2.1.1. *The compartments of the system (Equation* (2.3)*), with initial conditions (Equation* (2.4)*) have the following limits:*

$$\lim_{t\to\infty} y_i(t) = 0 \text{ for } i = 0, 1, \ldots, n-1,$$
$$\lim_{t\to\infty} y_n(t) = 100 \times 2^{n-3}.$$

The result of the proposition simply states that there are $n-3$ replication cycles. However, the model can accurately reproduce the empirical findings of the laboratory experiments, in particular, it can predict the number of EBs at any given time. Figure 2.2 shows that, after fitting our model parameters, we could generate time curves that match the laboratory measurements [7]. The fitting was done in Mathematica using the least square method, the codes for which can be found in the supplementary file available in our public GitHub repository [8]. As the plotting is done on a logarithmic scale, for the purpose of fitting we take the logarithm of the solution and fit the solution to the logarithm of the data values with respect to the parameters.

3 A Mathematical Model of Herpes and *Chlamydia* Co-Infection In Humans

A six-dimensional deterministic non-linear mathematical model is proposed in this section to analyze the transmission dynamics of *C. trachomatis* and herpes simplex virus (HSV) co-infection in human beings. The total population is denoted by $N(t)$ where,

$$N(t) = S(t) + C(t) + H(t) + I_{LC}(t) + I_{HP}(t) + L(t). \tag{3.1}$$

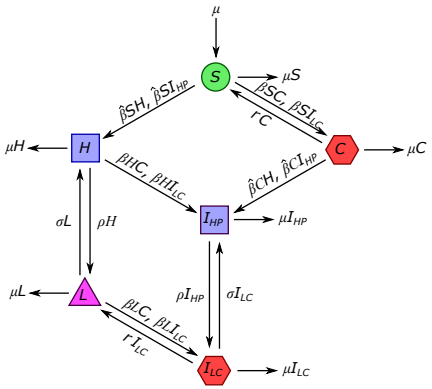

Figure 3.1: Schematic diagram for the *C. trachomatis*-HSV co-infection model.

With some assumptions about the interrelationship between the two pathogens, a description of variables given in Table 3.1, and parameters given in Table 3.2, the mathematical model can be formulated with the help of the schematic diagram given in Figure 3.1. In summary, the co-infection model consists of the following system of nonlinear ordinary differential equations:

$$\begin{cases} S' &= \mu - \beta SC - \hat{\beta} SH - \beta SI_{LC} - \hat{\beta} SI_{HP} - \mu S + rC, \\ C' &= \beta SC + \beta SI_{LC} - \hat{\beta} CH - \hat{\beta} CI_{HP} - rC - \mu C, \\ H' &= \hat{\beta} SH + \hat{\beta} SI_{HP} - \beta HC - \beta HI_{LC} - \rho H + \sigma L - \mu H, \\ I'_{LC} &= \rho I_{HP} + \beta LC + \beta LI_{LC} - r_c I_{LC} - \mu I_{LC} - \sigma I_{LC}, \\ I'_{HP} &= \hat{\beta} CH + \beta HC + \hat{\beta} CI_{HP} + \beta HI_{LC} - \rho I_{HP} - \mu I_{HP} + \sigma I_{LC}, \\ L' &= \rho H + r_c I_{LC} - \sigma L - \beta LC - \beta LI_{LC} - \mu L, \end{cases} \tag{3.2}$$

where $'$ denotes time-derivative, with non-negative initial conditions

$$P_0 = (S(0), C(0), H(0), I_{LC}(0), I_{HP}(0), L(0)) \in \mathbb{D}, \tag{3.3}$$

where

$$\mathbb{D} = \{(S, C, H, I_{LC}, I_{HP}, L) \in \mathbb{R}_+^6 \mid S + C + H + I_{LC} + I_{HP} + L = 1\} \tag{3.4}$$

is the natural state space, and is clearly positive invariant to the system Eq. (3.2).

Variables	Descriptions
$S(t)$	Number of population susceptible to both diseases
$C(t)$	Number of population infected with *C. trachomatis*
$H(t)$	Number of population infected with HSV
$I_{LC}(t)$	Number of population with latent HSV but active *C. trachomatis*
$I_{HP}(t)$	Number of population with active *C. trachomatis* but latent HSV
$L(t)$	Number of population with latent HSV

Table 3.1: Variables and their Descriptions

Parameters	Descriptions
β	transmission rate for *C. trachomatis*
$\hat{\beta}$	transmission rate for HSV
ρ	rate at which active HSV goes into latency
σ	rate at which latent HSV is activated
μ	natural death rate
r	recovery rate for *C. trachomatis*

Table 3.2: Parameters and their Descriptions

3.1 Analysis of the Co-infection Model

The analysis shows that the co-infection system (Equation (3.2)) has four equilibrium points: the disease free equilibrium point ($\mathcal{E}_S$), the *Chlamydia* present equilibrium point ($\mathcal{E}_C$), the HSV present equilibrium point ($\mathcal{E}_H$), the co-infection equilibrium point ($\mathcal{E}_{CH}$). Three important threshold values, the reproduction number for HSV ($\mathscr{R}_H$), the reproduction number for *Chlamydia* ($\mathscr{R}_C$), the reproduction number for *Chlamydia* at $\mathcal{E}_H$ ($\mathscr{R}_{CH}$), are obtained which determine the existence and the global stability of the equilibrium points. The threshold values are giveb by:

$$\mathscr{R}_C = \frac{\beta}{r+\mu} \text{ and } \mathscr{R}_H = \frac{\hat{\beta}(\mu+\sigma)}{\mu(\mu+\rho+\sigma)} \text{ and } \mathscr{R}_{CH} = \frac{\Delta_{11}}{\Delta_{12}},$$

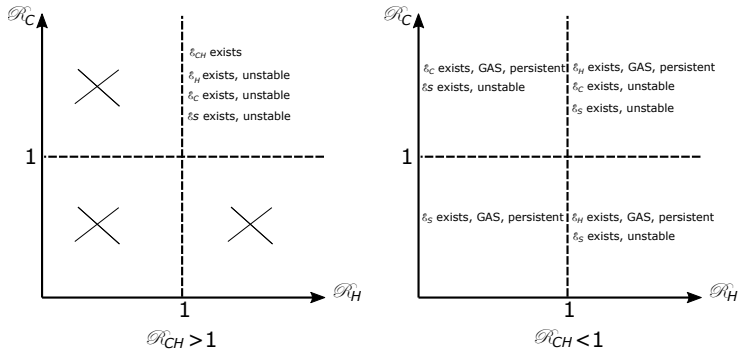

Figure 3.2: Existence and stability diagram of equilibrium points depending on $\mathscr{R}_C$, $\mathscr{R}_H$ and $\mathscr{R}_{CH}$. The global dynamics is fully described whenever $\mathscr{R}_{CH} < 1$. Cross-marks denote combinations of reproduction numbers that are not possible.

where

$$\begin{aligned}\Delta_{11} = [&\beta(\mu^5 + 3\mu^4(\rho+\sigma) + \hat{\beta}^2\rho\sigma(\rho+\sigma) + \hat{\beta}^2\rho\mu(\rho+3\sigma) + r(\rho+\sigma+\mu)\\ &\times(\mu^4 + 2\hat{\beta}\rho\mu + \mu^2(\rho+\sigma) + \hat{\beta}\rho(\rho+\sigma)) + \mu^3(-\hat{\beta}\rho + 3(\rho+\sigma)^2) + \mu^2\\ &\times(2\hat{\beta}^2\rho - \hat{\beta}\rho(\rho+\sigma) + (\rho+\sigma)^2))],\end{aligned}$$

and

$$\Delta_{12} = \left[\hat{\beta}(\rho+\sigma+\mu)((r+\mu)(\rho+\mu)+\sigma\mu)(\hat{\beta}(\sigma+\mu) + r(\rho+\sigma+\mu))\right].$$

Applying LaSalle's invariance principle, and the theory of asymptotically autonomous systems, the global asymptotic stability of two equilibria $\mathcal{E}_S$, $\mathcal{E}_C$ are proven. With a limiting system approach and theory of asymptotically autonomous systems, the global asymptotic stability of $\mathcal{E}_H$ is proven and the existence of a co-infection steady state is shown when all reproduction numbers are greater than one. The theorems are stated below.

Theorem 3.1.1. *Assume that $\mathscr{R}_H \leq 1$. If $\mathscr{R}_C \leq 1$, then the equilibrium point $\mathcal{E}_S$ is globally asymptotically stable, and if $\mathscr{R}_C > 1$, then $\mathcal{E}_C$ is globally asymptotically stable .*

Theorem 3.1.2. *The equilibrium point $\mathcal{E}_H$ is globally asymptotically stable if $\mathscr{R}_{CH} < 1$ and unstable if $\mathscr{R}_{CH} > 1$. In the latter case, a co-existing equilibrium $\mathcal{E}_{CH}$ exists.*

The results are summarized in the stability diagram Figure 3.2.

4 Optimal control for *Chlamydia* treatment with maturity-structured systems

We consider a compartmental maturity structured in-host model for intracellular development of *Chlamydia* taking into account its interactions with the immune system. Pontryagin's maximum principle is applied to determine the conditions for the most effective control to minimize systemic costs of the treatments/drugs, simultaneously minimizing the concentrations of extracellular Chlamydia, infected host cells, and persistently infected cells.

Variables	Descriptions
$C(t)$	Concentration of extracellular *Chlamydia* EBs
$I_1(t)$	Concentration of host cells infected with *Chlamydia* particles
$I_2(t)$	Concentration of infected cells with *Chlamydia* EBs transforming to RBs
$P(t)$	Concentration of cells infected with persistent *Chlamydia*
$A(t)$	Concentration of IFN-γ cells
$\rho(r,t)$	Concentration of host cells at time t that entirely contain replicating RBs, at the stage of maturity $r \in [0,R]$ over the replicating phase
$i(r,t)$	Concentration of host cells that contain RBs converting to EBs at the stage of maturity r
$u_1(t)$	Measure of the antibiotic concentration
$u_2(t)$	Measure of the tryptophan-L-1MT concentration

Table 4.1: Variables and their Descriptions

With some assumptions, description of variables given in Table 4.1 and parameters given in Table 4.2, the mathematical model can be formulated with the help of the schematic diagram given in Figure 4.1. In summary, the optimal control problem can be defined as:

$$\begin{cases} \dot{C}(t) & = (1-u_1(t))Nk_i(1)i(R,t) - \beta C(t) - \mu_C C(t), \\ \dot{A}(t) & = \omega I_1(t) - \mu_A A(t), \\ \dot{I}_1(t) & = (1-\theta)\beta C(t) - \alpha_1 I_1(t), \\ \dot{I}_2(t) & = \alpha_1 I_1(t) - \alpha_2 I_2(t) - \zeta A(t) I_2(t), \\ \rho(0,t) & = \alpha_2 I_2(t), \\ \frac{\partial \rho(r,t)}{\partial t} & = -\frac{\partial \left(k_\rho(r)\rho(r,t)\right)}{\partial r} - \zeta A(t)\rho(r,t), \\ \dot{P}(t) & = (1-u_2(t))\eta k_\rho(1)\rho(1,t) - \xi u_2(t) P(t) - \delta P(t), \\ i(0,t) & = (1-\eta)k_\rho(1)\rho(1,t) + \xi u_2(t) P(t), \\ \frac{\partial i(r,t)}{\partial t} & = -\frac{\partial (k_i(r) i(r,t))}{\partial r} - \zeta A(t) i(r,t), \end{cases} \tag{4.1}$$

where $r \in [0,1]$, $t \in [0,T]$. The initial conditions are

$$\begin{aligned} &C(0) = C_0, \\ &A(0) = I_1(0) = I_2(0) = I_3(0) = P(0) = I_4(0) = 0, \rho(r,0) = i(r,0) = 0. \end{aligned} \tag{4.2}$$

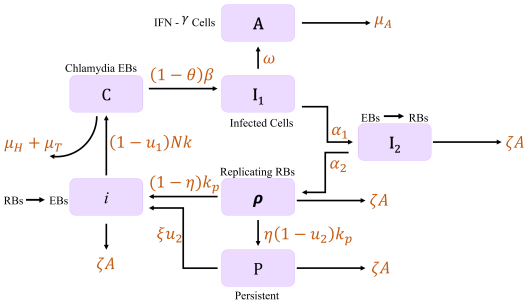

Figure 4.1: Schematic diagram for the *C. trachomatis* intracellular growth model with control.

Parameters	Descriptions	Values
β	Rate of attachment of *Chlamydia* particles into healthy epithelial cells	$2\,h^{-1}$[4]
μ_H	Humoral immunity induced death rate of extracellular EBs	$0.08\,h^{-1}$[4]
μ_T	Tryptophan-induced reduction in EB production	$0.04\,h^{-1}$[9]
ω	Production rate of IFN-γ cells	$0.001\,h^{-1}$ [10]
μ_A	Natural death rate of IFN-γ cells	$0.1\,h^{-1}$[10]
δ	Natural death rate of P	$0.1\,h^{-1}$
α_1	Rate of progression from I_1 to I_2	$0.125\,h^{-1}$[4]
α_2	Rate of progression from I_2 to the beginning of ρ	$0.1\,h^{-1}$[4]
η	Fraction of IFN-γ induced persistence	$0 \leqslant \eta \leqslant 1$
θ	Effect of attachment blocking due to humoral immune response	$0 \leqslant \theta \leqslant 1$
ζ	Rate of disintegration of *Chlamydia* infected cells by IFN-γ cell	$[0.05, 5]\,h^{-1}$ [10]
k	Rate of lysis of infected cells at the end of the cell cycle	$1.25\,h^{-1}$ [4]
m_1	Maximum dosage of control $u_1(t)$	0.9 [9]
m_2	Maximum dosage of control $u_2(t)$	0.9 [9]
ξ	Rate at which Tryp. reverses persistence	$0.6\,h^{-1}$[9]
N	Number of *Chlamydia* particles released upon cell lysis	$200-500$ [4]

Table 4.2: Parameters and their Descriptions

As the system (Equation (4.1)) is a maturity structured model, the results of the standard form of the Pontryagin's maximum principle that have been derived

for ordinary differential equations are not applicable. Hence, we construct an optimal control problem for a general compartmental model, where some of the compartments have maturity structure. Hence, it is a mixed system of ordinary and partial differential equations, moreover, the boundary conditions are also nonlinear. Subject to certain assumptions, for a fixed control, we verify the existence, uniqueness, and boundedness of the solutions. A suitable objective functional is formulated, and results for the presence of ideal control variables that minimize the objective function is determined. For the given system, we make use of Pontryagin's principle, which is a necessary condition for the optimality of the control. The Hamiltonian function, the adjoint variables and the corresponding differential equations along with transversality conditions are derived. In the proof, we considered the task as a constraint optimization problem, defined the Lagrangian functional, and derived the condition for its Fréchet derivative to be zero. As our results were proven for a general model with maturity structure, we believe that they can be applied to any particular compartmental model that is compatible with the system we have defined.

We consider an optimal control problem with the objective function given by

$$\begin{aligned} J(u) &= W_1 C^2(T) + W_2 I_1^2(T) + W_3 I_2^2(T) + W_4 P_2^2(T) \\ &\quad + \left(\int_0^1 (W_5(r)\rho(r,T) + W_6(r) i(r,T)) dr \right)^2 \\ &\quad + \int_0^T \Bigg(W_7 C^2(t) + W_8 I_1^2(t) + W_9 I_2^2(t) + W_{10} P_2^2(t) \\ &\quad + \left(\int_0^1 (W_{11}(r)\rho(r,t) + W_{12}(r) i(r,t)) dr \right)^2 + W_{13} u_1^2(t) + W_{14} u_2^2(t) \Bigg) dt. \end{aligned} \tag{4.3}$$

4.1 Numerical results

Using the forward-backward sweep method (FBSM), the optimal control strategy is numerically approximated [11, 12]. We look for the outcome that optimizes the usage of both the treatment types u_1, which acts as a bacteriostatic agent on *chlamydia*, and u_2 which stands for tryptophan-L-1MT supplement, with respect to two distinctive scenarios. We consider two different combinations of the weights as indicated in Table 4.3. According to our simulations, as detailed in Table 4.3 (a), the optimal control strategy advises maintaining the maximum concentration of the bacteriostatic agent, denoted as $u_1(t)$, throughout the entire treatment period. Likewise, for the tryptophan and L-1MT cocktail, referred to as $u_2(t)$, the optimal approach entails continuous administration, with the only exception being the discontinuation of $u_2(t)$ a few days prior to the conclusion of the treatment. This strategy is deemed effective in achieving the desired outcome. Next, we investigate for the weights in Table 4.3 (b). In this case, with the values of the weights as indicated in Table 4.3 (b), the optimal control predicts, as shown in Fig. 4.3b, Fig. 4.3c, and Fig. 4.5, by pri-

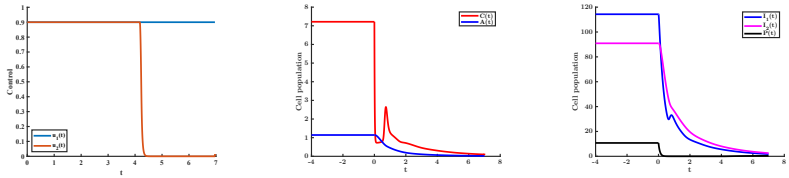

(a) (b) (c)

Figure 4.2: Numerical simulation for the control problem with the bacteriostatic agent and tryptophan-L-1MT supplementation for weights corresponding to Table 4.3 (a): (a) solution sketch for controls $u_1(t)$ and $u_2(t)$; (b) time course plot of state variables $C(t)$, and $A(t)$; and (c) time course plot of state variables $I_1(t)$, $I_2(t)$, and $P(t)$.

marily administering the bacteriostatic agent $u_1(t)$, and maintaining minimum concentration of tryptophan and L-1MT cocktail, *Chlamydial* elimination can be achieved. As depicted in Figure Fig. 4.3a, the optimal control strategy indicates that treatment should be administered using the highest concentration of u_1 for the entire duration of the treatment period, with some concentration of tryptophan and L-1MT cocktail administered before the end of therapy. In both cases, persistent *Chlamydia* have been successfully cleared from the system. In both cases, the commencement of the treatment period is $t = 0$, and it is seen that, before the initiation of the therapy, the disease remains at the chronic condition, which is the equilibrium point of the system.

	W_1	W_2	W_3	W_4	W_5	W_6
(a)	10	10	10	10	10	10
(b)	10	10	10	10	10	10
	W_7	W_8	W_9	W_{10}	W_{11}	W_{12}
(a)	1	1	1	1	1	1
(b)	0	0	0	0	0	0
	W_{13}	W_{14}				
(a)	10	5				
(b)	10	5				

Table 4.3: Table of weights

The primary distinction between the two control types lies in their effect on the persistent *Chlamydial* load within the system throughout the course of therapy. In the initial scenario, as illustrated in (Fig. 4.2c), it is evident that the control measures effectively and promptly eliminate the persistent *Chlamydia* from the system. In the second scenario, when the weights W_i for $i = 7, 2, \ldots, 12$ are not factored into consideration, the model forecasts a prolonged duration for the treatment to effectively eradicate the persistent *Chlamydial* particles from the system. This is visually represented in Figure (Fig. 4.3c).

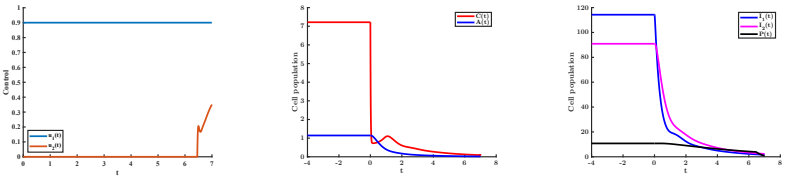

(a) (b) (c)

Figure 4.3: Numerical simulation for the control problem with the bacteriostatic agent and tryptophan-L-1MT supplementation for weights corresponding to Table 4.3 (b): (b) solution sketch for controls $u_1(t)$ and $u_2(t)$; (b) time course plot of state variables $C(t)$, and $A(t)$; and (c) time course plot of state variables $I_1(t)$, $I_2(t)$, and $P(t)$.

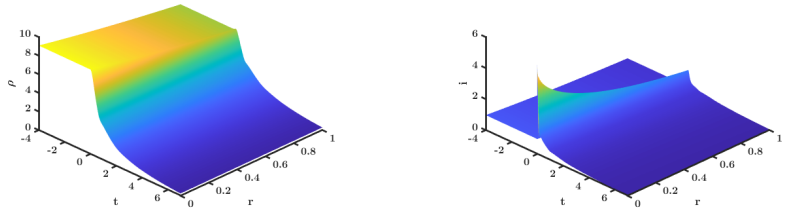

(a) (b)

Figure 4.4: Numerical simulation for the control problem with a bacteriostatic agent and tryptophan-L-1MT supplementation for weights corresponding to Table 4.3 (a): (a) time course plot of state variable $\rho(r,t)$; and (b) time course plot of state variable $i(r,t)$.

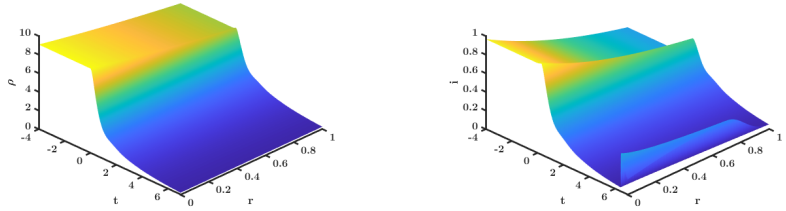

(a) (b)

Figure 4.5: Numerical simulation for the control problem with bacteriostatic agent and tryptophan-L-1MT supplementation for weights corresponding to Table 4.3 (b): (a) time course plot of state variable $\rho(r,t)$; and (b) time course plot of state variable $i(r,t)$.

Bibliography

[1] C. Kaushic, A. D. Murdin, B. J. Underdown, and C. R. Wira. “Chlamydia trachomatis infection in the female reproductive tract of the rat: influence of progesterone on infectivity and immune response”. *Infection and immunity* 66.3 (1998), pp. 893–898.

[2] WHO. *Global incidence and prevalence of selected curable sexually transmitted infections-2008*. World Health Organization, 2012. URL: https://iris.who.int/bitstream/handle/10665/75181/9789241503839_eng.pdf.

[3] H. Weinstock, S. Berman, and W. Cates Jr. “Sexually transmitted diseases among American youth: incidence and prevalence estimates, 2000”. *Perspectives on Sexual and Reproductive Health* 36.1 (2004), pp. 6–10.

[4] D. Wilson, P. Timms, and D. McElwain. “A mathematical model for the investigation of the Th1 immune response to Chlamydia trachomatis”. *Mathematical Biosciences* 182.1 (2003), pp. 27–44.

[5] Y. M. AbdelRahman and R. J. Belland. “The chlamydial developmental cycle”. *FEMS Microbiology Reviews* 29.5 (2005), pp. 949–959.

[6] R. Schoborg. “Chlamydia persistence–a tool to dissect chlamydia–host interactions”. *Microbes and Infection* 13.7 (2011), pp. 649–662.

[7] K. Siewert, J. Rupp, M. Klinger, W. Solbach, and J. Gieffers. “Growth cycle-dependent pharmacodynamics of antichlamydial drugs”. *Antimicrobial Agents and Chemotherapy* 49.5 (2005), pp. 1852–1856.

[8] B. Das and G. Röst. *GitHub 2023, Supplementary Codes for Delay Linear Chains in Mathematical Biology: An Insight into the Intracellular Chlamydia Infection*. 2023. URL: https://github.com/Epidemic-Models/Epidemic-Models-delay_linear_chain_chlamydia_fitting_mathematcia.

[9] M. D. Akinlotan, D. G. Mallet, and R. P. Araujo. “An optimal control model of the treatment of chronic Chlamydia trachomatis infection using a combination treatment with antibiotic and tryptophan”. *Applied Mathematics and Computation* 375 (2020), p. 124899.

[10] O. Sharomi and A. Gumel. “Mathematical study of in-host dynamics of Chlamydia trachomatis”. *IMA Journal of Applied Mathematics* 77.2 (2012), pp. 109–139.

[11] S. Lenhart and J. T. Workman. *Optimal control applied to biological models*. Chapman and Hall/CRC, 2007.

[12] M. McAsey, L. Mou, and W. Han. “Convergence of the forward-backward sweep method in optimal control”. *Computational Optimization and Applications* 53 (2012), pp. 207–226.